SUBMITTED PAPER

Parametric study of the mixing efficiency in a kneading block section of a twin-screw extruder.

B. Alsteens[1], V. Legat[1], Th. Avalosse[2]

June 29, 2004

(1) University of Louvain, Center for Systems Engineering and Applied Mechanics (CESAME) Av. Georges Lemaître, 4, B-1348 Louvain-la-Neuve, Belgium.

(2) Fluent Benelux, Av. Pasteur, 4, B-1300 Wavre, Belgium.

1

Abstract

Twin-screw extruders are often used to distribute and disperse additives into polymers. The mixing efficiency of the extruders highly depends on the geometry of the kneading blocks of the mixing section. In this paper, the impact of some geometrical parameters, such as the stagger angle and the width of the discs, are investigated by three dimensional time dependent finite element calculations.

Results are obtained with the finite element software POLYFLOW. The robustness and the accuracy of the *mesh superposition technique* is evaluated. It appears that conclusions obtained by the numerical experiments can be used to improve the geometry of the kneading blocks. The mixing efficiency is evaluated by comparing the residence time and the total shear distributions of a large set of virtual particles launched in the flow domain.

Introduction

In plastic, rubber and food industry, the mixing of raw materials is a critical step of the process. The morphology and the specific properties of the final product depends on the uniformity of the mixture and therefore on the quality of the mixing. In the literature, a distinction is usually made between the dispersive and distributive mixing [1]. On one hand, the distributive mixing consists of creating a flow kinematics that will provide a uniform concentration of all components. On the other hand, the dispersive mixing consists of breaking clumps or aggregates into particles of the smallest size as possible. Both goals can be achieved simultaneously or in several steps. In most cases, twin-screw extruders are used to distribute and disperse additives into polymers. The dispersive mixing is obtained by the shear and elongational stresses created, while the distributive mixing is achieved by frequent stretching and reorientations of the flow. Each element of the extruders (including some part of the feed or the devolatization section, for instance) can dramatically affect the quality of the final product. However, the kneading block of the mixing section of the twin-screw extruders is the most important element. A kneading block is a discontinuous unit mainly composed of several discs. The mixing efficiency of the extruder highly depends on the geometry of such kneading blocks. In this paper, we use the numerical simulation to analyze the sensibility of some typical parameters characterizing this geometry : the stagger angle, the width and the number of discs [2].

Previous experimental and numerical investigations were performed in several contributions in the literature. In 1964, Erdmenger [3] has first described the flow mechanism in the kneading disc region. He observed a forward drag flow when the kneading discs have a right-handed stagger angle and a backward leakage flow through the tips of the kneading discs. Other flow visualizations were reported by Sastrohartono et al. [4], Bigio et al. [5], Todd [6] and Kim et al. [7]. More recently, Bakalis et al. [8] [9] used the laser Doppler anemometry to investigate local feature of the flow. However, such experimental approaches are very expensive, time consuming and only provide a partial information: it is almost impossible to extract all local information. The main advantage of the numerical and virtual laboratories is the possibility to provide all local information at any position of the twin-screw extruder. Of course, it is the information related to a mathematical model that is only an approximation of the reality. A large number of contributions in the literature demonstrate that the numerical approach seems to be a useful tool to study mixing devices.

In 1980, Booy [10] already proposed one-dimensional model and extracted

averaged values of the pressure in the flow direction. More recent contributions of Lozano et al. [11] [12] demonstrate that those simplified 1D models are still a very interesting way. In 1987, Szydlowski presented bidimensional results obtained by means of the flow analysis network [13]. The flow in the radial direction is neglected and a two dimensional mesh is build in a three dimensional reference. Such an approach is very popular, as illustrated by some people : Speur et al. [14], Gotsis et al. [15], Bigio et al. [16] and Potente et al. [17]. It allows to keep some local features. Nevertheless, in an extruder we have a three dimensional time dependent flow, and to catch all information, a three dimensional time dependent calculation is required.

Three-dimensional calculations have been recently reported in the literature. In 2000, Yoshinaga et al. [18] and Ishikiwa et al. [19] reported such results by generating a new mesh for each position of the screws at each time step. Time dependent fields are then obtained by interpolation between the meshes. But this method requires a huge tedious meshing work or very complex meshing tools. Good agreement between numerical and experimental results in terms of velocity and pressure profiles have been obtained by Bravo et al. [20] [21] in 2000. Ishikawa et al. [22] investigate the impact of different combinations of kneading blocks on the mixing efficiency of a twin-screw extruder in 2001. As suggested by Rios et al. [23], the boundary element method offers an alternative to the meshing effort but incorporating non-linearity of a rheological model is a very tedious issue. In this paper, we use a constrained finite element formulation for non-conforming meshes. Using a penalty technique, it allows us to avoid the complex task of meshing the flow domain. In this so-called *mesh superposition technique* [24], we only need to mesh the inner part of the barrel and each screw in an independent way. The position of the screws mesh is updated at each time step. For each node of the barrel mesh, we must detect if the node is inside the screws and if its velocity has to be constrained. In the other case, the velocity is computed by solving the Navier-Stokes equation. This technique can be directly compared to the *fictitious domain method* used by Bertrand et al. [25]. They impose the kinematics constrains by means of Lagrange multipliers and not by a penalty technique.

Nevertheless, those simulations remain challenging due to the complexity of the three dimensional time dependent flow pattern. Therefore, it is required to carefully evaluate the robustness and the accuracy of the calculation : the sensibility of the numerical parameters, the rheological model and the operating conditions are investigated in this paper. Finally, several three dimensional time dependent results are presented to analyze the flow patterns generated by different configurations of kneading blocks. Their mixing

efficiency is evaluated in comparing the residence time, the maximum shear rate and the total shear distributions of a set of virtual particles launched in the flow domain.

Mathematical Modeling

Let us consider a time-dependent isothermal and incompressible flow of a generalized Newtonian fluid. The governing partial differential equations thus read:

$$\begin{cases} \rho \, \dfrac{D\mathbf{v}}{Dt} & = \quad -\boldsymbol{\nabla}p + \boldsymbol{\nabla}\cdot\boldsymbol{\tau} + \rho\,\mathbf{g} \\[2ex] \boldsymbol{\nabla}\cdot\mathbf{v} & = \quad 0 \end{cases} \tag{1}$$

where D/Dt is the material derivative, $\mathbf{v}$ is the velocity, p is the pressure, ρ is the density, $\mathbf{g}$ is the gravity and $\boldsymbol{\tau}$ is the extra-stress tensor defined by:

$$\boldsymbol{\tau} = 2\eta(\dot{\gamma})\mathbf{d}$$

with the strain rate tensor $\mathbf{d}$ and the kinematic viscosity η. The shear rate $\dot{\gamma}$ is defined as the square root of the second invariant of the strain rate tensor,

$$\dot{\gamma} = \sqrt{2\mathbf{d}:\mathbf{d}}$$

As we consider flows in a twin-screw extruder with a rotational speed of 250 rpm and a flow rate of 0.02 kg/s, we are dealing with $Re \sim 10^{-2}$ and $Re/Fr \sim 10^{-1}$. In other words, we consider creeping flow assumption and neglect gravity effects.

To build a mathematical model of the mixing process of a polyamide in a twin-screw extruder, several geometrical assumptions and a simplified constitutive model for the fluid are selected [1]. Even if three dimensional geometrical issues are very important, a correct balance between the complexity of the geometrical model and the complexity of the rheological model has to be identified. It is useless to use a complex rheological model with a relatively coarse geometrical discretization. It is also useless to consider irrelevant geometrical details with a very poor rheological model. The cost of large time-dependent three-dimensional calculations and the numerical accuracy that can be obtained have to be taken into account to get a suitable

compromise between the numerical and the modeling error. In view of the geometrical assumptions that we have to introduce, it seems reasonable to reproduce only the shear thinning behavior of the polyamide by a Bird-Carreau model [26] [27] :

$$\eta(\dot{\gamma}) = \eta_0 \left(1 + (\lambda\dot{\gamma})^2 \right)^{(n-1)/2} \tag{2}$$

where $\eta_0 = 313\ Pas$ is the zero shear rate viscosity, $\lambda = 0.0025\ s$ is a natural time and $n = 0.5$ is the power law index. Those parameters have been selected to fit experimental measurements at a temperature of $250°C$ as illustrated in Figure 1. The density of this polyamide is $969\ kg/m^3$.

As the goal of the paper is not to analyze the interaction between several combinations of kneading blocks, but to focus on the geometrical design of one kneading block, the analysis will be restricted to one kneading block composed of five or ten discs, as shown in Figure 2. As one major advantage of such an approach, we are allowed to consider only isothermal flow because the increase of temperature observed along only one kneading block is quite small in the considered operating condition. To be able to set boundary conditions, we add to the computational domain some sufficiently long inlet and outlet channels where fully developed flows can be assumed. Therefore, a developed velocity profile is imposed at the inlet section and vanishing normal velocity and tangential force are imposed as usual at the exit section. The dimensions of the computational domain are given in Table 1. Along the barrel and the screws, a full sticking condition is imposed. It is a strong assumption, as most people observe partial slipping of the polymer along the screws and the barrel. However, some experiments suggest that a sticking condition is a better approximation of the reality. Finally, as the amount of the slipping along the screws is still an open question deserving a full analysis, it seems to be fair to restrict ourselves to a stick condition. Finally, the mixing section of the twin-screw extruder is assumed to be fully-filled because the numerical simulation of a partially filled domain requires both extremely sophisticated algorithms and prohibitive cost.

As we mainly wish to analyse the impact of the geometrical design of a kneading block on the flow, let us briefly recall how the geometrical construction of the screw cross section is performed. Basically, the geometry of a kneading block depends on the following parameters [2]:

- the *number and width* of the discs. In this analysis, we consider kneading blocks of five or ten discs, with a width of 8 *mm* or 4 *mm* respectively. The total width is always 40 *mm*.

- the *stagger angle* ϵ between the discs. Typically, we consider the so-called neutral, pump and reverse elements with stagger angles of 90°, 45° and −45° respectively.

- the *geometry* of the cross-section of the disc. To build the cross-section of the disc, let us use the same construction as M.L. Booy [28]. A unique shape for the cross-section of the disc can be defined from a radius R_e, a centerline distance L and a number of tips. In Figure 3, let us restrict ourselves to a cross-section with two tips. We draw two circles Γ_e and Γ_i with the same center O and radius equal to R_e and $R_i = L - R_e$ respectively. From an arbitrary point A of Γ_e, we define points B and C lying on Γ_e such that the angle $AOB = \frac{\pi}{2}$ and the distance $AC = L$, respectively. The right limit P of the upper tip is then located midway between B and C. Other limits of tips are located symmetrically to the axis OA and OB. Finally, the shape of the flank curve is an arc PF of circle Γ_f whose the radius is L and the center D is lying of Γ_e such that the distance $DP = L$. The point F is defined as the intersection of circles Γ_f and Γ_i. The last part of the cross section is defined as the root curve that is the arc FF' of the circle Γ_i. The numerical parameters of the cross-section used in this analysis are given in Table 2.

In the mixing of two immiscible polymers, we observe droplets or filaments of one component in the other one. The evolution of those filaments is the result of the combination of the shear stress applied by the flow field and the interfacial force [29]. At a given time, both effects are in competition at a local level and lead to the break-up into smaller droplets. Deformations can be, approximately, considered as proportional to the total shear. It is required that the filament experiences folding and reorientation several times to observe an exponential increase of the stretching and to guarantee a good mixing efficiency : the well known baker's transformation is the classical exemple of such a requirement. In this study, we will thus estimate the mixing efficiency by the evolution of the total shear, the shear rate and the residence time of a particle in the flow domain. In order to obtain a global stretching efficiency, we also evaluate the ratio between the energy converted into stretch and the mechanical energy dissipated in the flow. This ratio, so-called global stretching efficiency, is calculated from the logarithm of the area stretch ratio and from the strain rate tensor [30].

Obviously, those measures provide a limited insight. Other indicators (the scale of segregation, the mapping method matrix, the distributive index,...)

[31] [32] [33] and micro-macro modeling of the dispersive mixing are required if we wish to get a better understanding of the process.

Numerical Techniques

To perform simulations, we use a finite element software dedicated to highly viscous flows: POLYFLOW [34]. In order to get reliable results, a fine design of the mesh and a suitable selection of the mixed interpolations remain critical.

Mesh refinement analysis

In general, the design of the mesh between the barrel and the screws is a very tedious task that has to be repeated for each position of the screws in a transient simulation. In the *mesh superposition technique* [24], used in this analysis, we independently build the mesh of the flow domain and the mesh of each screw. The mesh of the flow domain and the screws are then superimposed as illustrated in Figure 4. The position of the screws is updated at each time step. It is finally required to detect if the node is included in one of the two screws or in the actual "fluid" region. Outside the screws, the velocity of the node is calculated by satisfying the weak formulation of the Navier-Stokes equations. Otherwise the velocity of the node is constrained at the velocity of the screws.

This technique presents two major advantages. Firstly, only two meshes without complex intermeshing regions have to be built to perform a transient simulation. Secondly, the method is efficient and robust thanks to the absence of remeshing algorithm. Nevertheless, the accuracy of this method is lower than the accuracy of a classical method and requires a mesh refinement. Obviously, if the mesh becomes too coarse in some areas, very poor numerical results can be obtained. Typically, the mass conservation cannot be always guaranteed; fluid leakage can appear in some critical parts of the flow domain. Such a bad behavior comes from the penalty formulation used in the mesh superposition technique that is not formally a conservative numerical technique: we have thus to maintain the mass conservation under control. The local loss of the mass conservation can modify in a significant way the flow features.

To maintain an acceptable numerical cost, a first coarse mesh of $15,570$ bricks for the flow domain is built. Nevertheless, it is already a quite costly

calculation and it prohibits performing a classical mesh refinement analysis uniformly in all the directions. Therefore, we restrict ourselves to the radial and axial direction, keeping the same azimuthal distribution. Medium and refined meshes are thus defined with $22,550$ and $32,220$ bricks.

Convergence analysis is performed by comparing the pressure evolution along the line AA' illustrated in Figure 2 and defined in Table 1. In Figure 5, the pressure profiles strongly depend of the mesh refinement. Basically, we observe convergence of the results especially between the two more refined meshes. As expected, obtaining a fully converged value for the pressure peak remains a critical issue and quite more difficult than for the velocity field. The radial direction is the most critical. As the use of a direct frontal solver renders radial refinement quite costly, the medium mesh can be viewed as a compromise between the number of degrees of freedom and the required accuracy.

Selection of the mixed interpolation

For the Stokes problem, it is well known that the interpolation of the velocity and pressure has to satisfy the Brezzi-Babuska condition [35] for a usual Galerkin formulation as used in the software. Otherwise, a stabilized pressure Petrov Galerkin formulation could be used with an equal-order approximation. Moreover, in our specific application, the penalty technique applied on the flow bricks partially superimposed by the screws, requires special care because locally the ratio between velocities and pressure unknowns is modified in the wrong way for the stability issue. We investigate three mixed interpolations defined in Figure 6.

- $Q_1 - Q_0$: hexahedral linear velocity and constant pressure interpolations. Such an element is widely used in a large number of applications even if it does not formally satisfy the BB condition.

- $Q_1^+ - Q_0$: mini-element velocity and constant pressure interpolation. The velocity interpolation is a usual hexahedral linear element at which a scalar degree of freedom is added in each face.

- $Q_1^{++} - Q_1$: enriched mini-element velocity and linear pressure interpolation. An additional bubble function enriches the velocity field to define Q_1^{++} element from Q_1^+ element.

The solutions for the same problem solved with the three elements are compared in Figure 7. A similar pressure drop between the inlet and the

outlet channel is obtained with both $Q_1^{++} - Q_1$ and $Q_1^+ - Q_0$ interpolations. Nevertheless, we observe some spurious oscillations with $Q_1^{++} - Q_1$ interpolation and an underestimated pressure drop with $Q_1 - Q_0$ element. The best compromise between the numerical cost and the accuracy seems to be addressed by the $Q_1^+ - Q_0$ element for a given mesh. The other mixed interpolations are too expensive or not very accurate.

Finally, the cost of a simulation with the medium mesh and the $Q_1^+ - Q_0$ interpolation remains important. A transient simulation takes around 14 hours for 26 times steps and requires 1387 Mbytes of memory on a DEC Alpha server (600Mhz-1Gb of memory).

Measure of the mixing quality and efficiency

To evaluate the mixing provided by each kneading block, a very large number of virtual particles are launched at the same time in the flow domain. Initially, those particles are randomly distributed in an inlet vertical plane and their trajectory is calculated from the velocity field [36]. The flow pattern is assumed to be not affected by the occurence of particles. Such an assumption is relevant if the concentration of the minor component in the major one is very small.

A characteristic residence time for all particles can be estimated from a characteristic flow rate, mixing length and the area of the flow section. If a particle does not leave the flow domain after forty times such a characteristic residence time, its history is disregarded for our analysis (typically 16 seconds). Typically, theses particles stick to either the barrel or the screws. Their axial velocity vanishes and they never reach the end of the mixing section. In order to deliver reliable statistics about mean residence time needed to reach the exit section and othe global feature of the trajectories, it is essential that all the trajectories used in the mixing analysis reach the end of the mixing section. Nevertheless, the number of particles that sticks to the barrel or to the screws can be also representative of the complexity of the channels created by the motion of the screw. Along each trajectory, we evaluate current elapsed time, the shear rate and the total shear.

The next step consists in defining three planes : α, β and γ as shown in Figure 8. In each plane, the distributions of residence time and total shear of particles crossing this plane are calculated. For example, let us consider that we wish to obtain the distribution of the residence times required to reach the plane α. We take into account the first intersection between each trajectory and the plane. Considering only the first intersection avoids to give

much weight to a particle crossing several times the same plane, as illustrated by the trajectory Γ_3. By collecting all residence time of the particles, it is thus possible to estimate the residence time distribution for this plane α. The distribution represents the frequency with which particles with a given residence time in the global population can be found.

Basically, most distributions are characterized by three parameters defined in Figure 9. For the residence time, for example, we consider the following parameters : the smallest time observed in a given plane, the time needed by 75% of the particles to reach the plane and the difference between both previous values. Those parameters are denoted T_{min}, T_{75} and $\Delta T = T_{75} - T_{min}$, respectively.

Sensibility analysis

Now, we are able to analyse the effect of the material and of the kneading block geometry on the mixing. More precisely, we investigate the impact of the stagger angle and the disc width. In Figure 10, we consider three kneading blocks composed of five discs with a stagger angle of 90°, 45° and −45° respectively and one element with 10 discs and a stagger angle of 90°. Stagger angles of 90°, 45° and −45° usually define neutral, pump and reverse elements.

Effect of the rheological model

The impact of the material on the flow is estimated by modifying the effect of the shear thinning behavior of the model. Three simulations with three different values of the power law index ($n = 0.6$, 0.7 and 1) are performed with the neutral element composed of five discs.

In Figure 11, the peaks of pressure, in the intermeshing zones, decreases with the power law index. It is in those clearance and intermeshing zones that the high shear rate leads to significant change of viscosity in the non-Newtonian model. Differences in the pressure fields only appear in those areas that are quite small in comparison with the whole flow domain. In other words, the global pressure drop between the inlet and the outlet section is not significantly affected by the rheological model. As the use of a Bird-Carreau law model significantly increases the cost of the calculation without any major difference in the flow features, it seems attractive to use only a Newtonian model with a constant viscosity of $313 Pas$. Such a conclusion is

only valid for a relatively moderate flow rate and has to be revisited if we dramatically change the operating conditions.

Effect of the stagger angle and disc width on the mixing quality and mixing efficiency

Firstly, let us compare the flow patterns in terms of pressure for all kneading blocks. The pump element drags the fluid across the mixing section from the inlet, the pressure exhibits a progressive increase of 5 bars. On the other hand, the reverse element tends to create a flow in the opposite direction and a pressure decrease of 10 bars is now observed. Finally, for the same number of discs, the neutral element exhibits the smallest pressure drop of 2.5 bars. Increasing the number of discs for the same length only generates a slightly higher pressure drop of 3 bars, due to the higher number of reorientations of the flow.

In the mixing section of the screw, the shear rate distribution can be estimated by sampling some particles. Distribution with moderate, high and very high shear rate are given in Figure 12. Typically, all mixing elements provide similar distributions. However, in term of maximum shear rate experienced by the particles, we observe in Table 4 that the neutral element with 10 discs is sharing the best performance with the reverse element. Such an observation can be directly linked to the ability to perform dispersive mixing.

The next information that we extract from our calculations is the time distribution given in the Figure 13 and in Table 4. We present the distributions of the time required by the particle to reach the planes α, β and γ respectively. Differences progressively appear when we enter deeper in the mixing section from the plane α to the plane γ. The flow in the opposite direction created by the reverse geometry makes more difficult the crossing of the mixing section by the particles that need a larger time to reach the last plane γ. Surprisingly, we do not observe any major difference between the pump and neutral element with five discs. Finally, a larger number of discs strongly increases the residence time by a larger number of reorientations of the flow. For the same length, the neutral element with 10 discs generates the longest residence time.

The most critical distributions for the distributive efficiency are the total shear distributions given in Figure 14. To reach a high total shear, a particle must have a high residence time or exhibit a very high shear rate. Combination of both effects is obviously the best case obtained by the reverse

geometry for the same number of discs. However, increasing the number of discs improves the situation by increasing the residence time.

We conclude that the reverse geometry and a larger number of discs increase the mixing quality. Nevertheless, if we take into account the energy the best compromise is obtained by the neutral element with five discs as predicted by the global stretching efficiency given in Table 4. The final selection of the best candidate will be guided by energetic considerations and mechanical constraints as the total length of the screws.

Finally, good quality of distributive and dispersive mixing is not achieved if we do not obtain homogeneous distributions of the properties of the final compound. Typically, large distribution of total shear or residence time is the sign of inhomogeneities and has to be avoided. In other words, we wish that all matter exits the mixing section with the same prescribed residence time, total shear and maximum shear stress. Unfortunately, the element providing the highest total shear also exhibits the largest distributions. In contrary, the pump and neutral element provide a more homogeneous product (Table 5).

Conclusion

The mixing of different compounds is a key step of extrusion processes. The quality of the final product obtained with a twin-extruder depends mainly on the dispersive and distributive mixing generated by the kneading blocks. We have used here the numerical simulation to understand the impact of two classical geometrical parameters on the mixing: the stagger angle and the number of discs. From our calculations, we are able to rank four typical kneading blocks. Our conclusions from the numerical experiences appear to be in very good agreement with global classical interpretation of the flow [37]. It is also in line with guidelines found in reference books. Extension of such a sensibility analysis to other geometrical parameters is straightforward.

We observe that the finite element simulations are an efficient tool to understand complex mixing features and allows us to extract global and local information. Such data are almost inaccessible by the experimental approach. Finally, we demonstrate that several useful approximations for the rheological model and for the mesh design can be introduced. Those approximations are essential to keep the numerical cost of three dimensional transient calculation reasonable. It is also mandatory to check that physical relevance and suitable accuracy are still obtained in the simulation. Such a compromise is still a difficult task even if you are using a certified numerical software.

References

[1] Meijer, H.E.H. : Material Science and Technology, A comprehensive Treatment 18. Wiley Publishers (1997).

[2] Todd, D.B. : Plastic Compounding Equipment and Processing, Hanser Publishers, Munich(1998).

[3] Erdmenger, R., Chem. Ing. Tech., 36, p.175(1964).

[4] Sastrohartono, T., Esseghir, M., Kwon, T., Sernas, V., Polym. Eng. Sci. 30, p.1382(1990).

[5] Bigio, D., Stry, W., Polym. Eng. Sci. 30, p.153(1990).

[6] Todd, D.B., Inter. Polym. Proc. VI,p.143(1991).

[7] Kim, P.J., White, J.L., Inter. Polym. Proc. IX, p.108(1994).

[8] Chandrasekaran, M., Marcroft, H., Bakalis, S., Karwe, M.V., Trends in Food Sc. Technol. 8, p.369(1997).

[9] Bakalis, S., Karwe, M.V., J. Food Eng. 51, p.273(2002).

[10] Booy, M.L., Polym. Eng. Sc. 20 (18), p.1220(1980).

[11] Lozano, T., Lafleur, P.G., Grmela, M., Vergnes, B., Intern. Polym. Processing 18, p.12(2003).

[12] Lozano, T., Lafleur, P.G., Grmela, M., Vergnes, B., Polym. Eng. Sci. 42, p.347(2002).

[13] Szydlowski, W., Brzoskowski, R., White, J.L., Int. Polym. Process. 1, p.207(1987).

[14] Speur, J.A., Mavridis, H., Vlachopoulos, J., Janssens L.P.B.M., Adv. Polym. Tech. 7, p.39(1987).

[15] Gotsis, D., Kaylon, D.M., SPE ANTEC Tech. Papers 35, p.44(1989).

[16] Bigio, D., Zerafati, S., Polym. Eng. Sc. 31, p.1400(1991).

[17] Potente, H., Flecke, J., Proc. 55th Annu. Tech. Conf. SPE, p.110(1997).

[18] Yoshinaga, M., Katsuki, S., Miyazaki, M., Liu, L., Kihara, S., Funatsu, K., Polym. Eng. Sc. 40(1), p.168(2000).

[19] Ishikiwa, T., Nagashima, Y., Funatsu, K., Polym. Eng. Sc. 40(2), p.357(2000).

[20] Bravo, V.L., Hrymak, A.N., Wright, J.D., Polym. Eng. and Sc. 40(2), p.525(2000).

[21] Shaffiqa, J., Bravo, V.L., Wood, Ph., Hrymak, A.N., Polym. Eng. and Sc. 40(4), p.892(2000).

[22] Ishikawa, T., Kihara, S., Funatsu, K., Polym. Eng. Sc. 41(5), p.840(2001).

[23] Rios, A.C., Osswald, T.A., Eng. Analysis Boundary Element 24, p.89(2000).

[24] Avalosse, Th., Rubin, Y., Intern. Polym. Processing 15(2), 2000.

[25] Bertrand, F., Thibault, F., Delamare, L., Tanguy, P.A., Comput. Chem. Eng. 27, p.491(2003).

[26] Barnes, H.A., Hutton, J.F., Walters, K. : An Introduction to Rheology. Elsevier, Amsterdam(1989).

[27] Macosko, C.W. : Rheology:principles, measurements, and applications. New York(1994).

[28] Booy. M.L., Polym. Eng. Sc. 18(12), p.973 (1978).

[29] Manas-Zlocsower, I., Tadmor, Z. : Mixing and Compounding of Polymers, Theory and Practice. Hanser Publishers, Munich (1993).

[30] Ottino J.M. : The Kinematics of mixing: stretching, chaos and transport. Cambridge university Press, Cambridge (1989).

[31] Danckwerts, P.V., Appl. Sc. Res. A3, p.279(1951).

[32] Galaktionov, O.S., Anderson, P.D., Kruijt, P.G.M., Peters, G.W.M., Meijer, H.E.H., Comput. Fluids 30, p.271(2001).

[33] Avalosse, Th., Macromol. Symp. 112, p.91(1996).

[34] Debbaut, B., Keunings, R., Crochet, M.J., Proc. Europ. Conf. New Adv. Comput. Struct. Mech., p.689(1991).

[35] Brezzi, F., Fortin, M. : Mixed and hybrid finite elements methods. Springer, New York(1991).

[36] Avalosse, Th., Crochet, M., AIChE J. 43 (3), p.577(1997).

[37] Carneiro, O.S., Poulesquen, A., Covas, J.A., Vergnes, B., Intern. Polym. Process. 17, p.301 (2002).
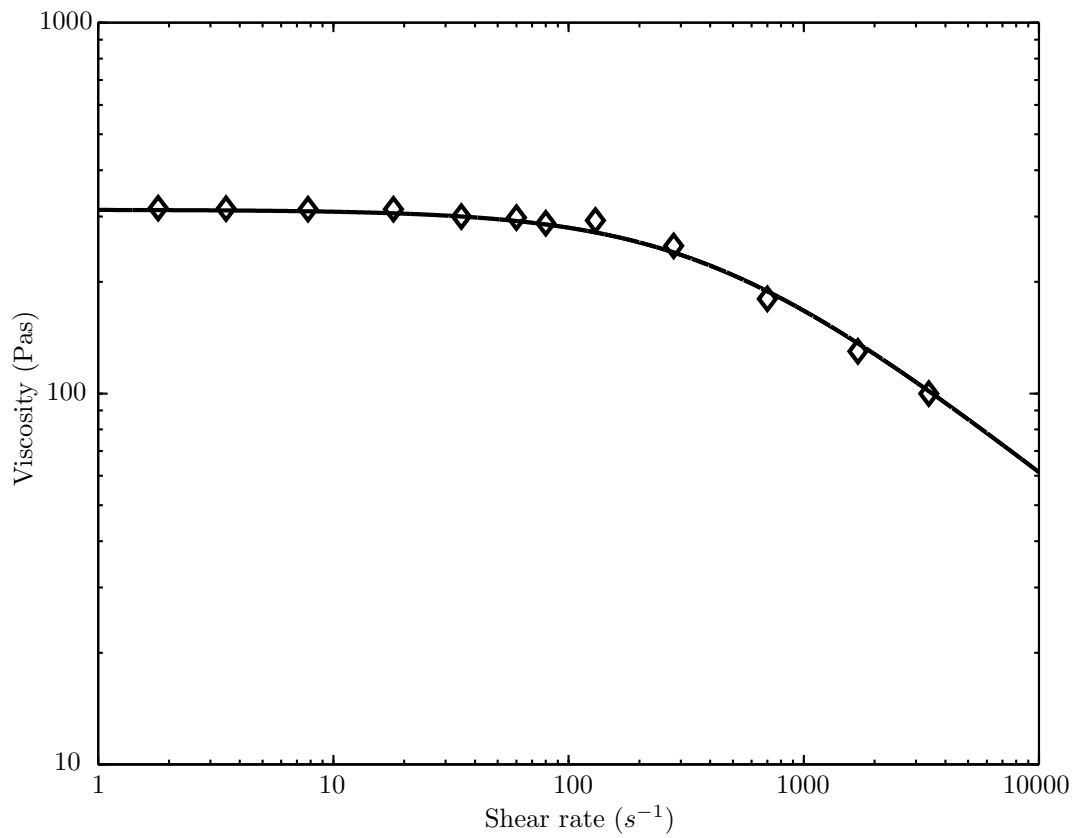
Figure 1: Viscosity of the polyamide vs. shear rate ($\diamond$) at a temperature of $250°C$. Experimental data and fitted curve result obtained with Bird-Carreau law (solid line).
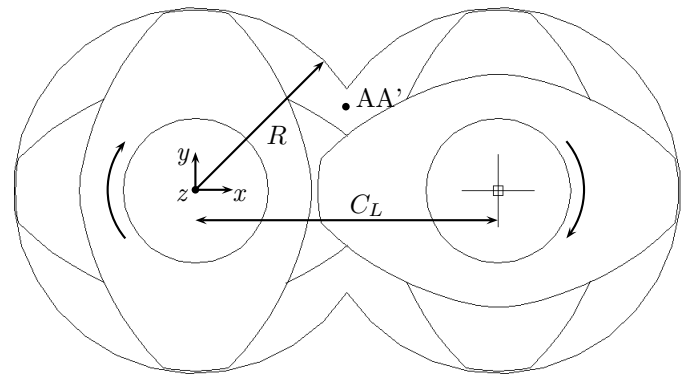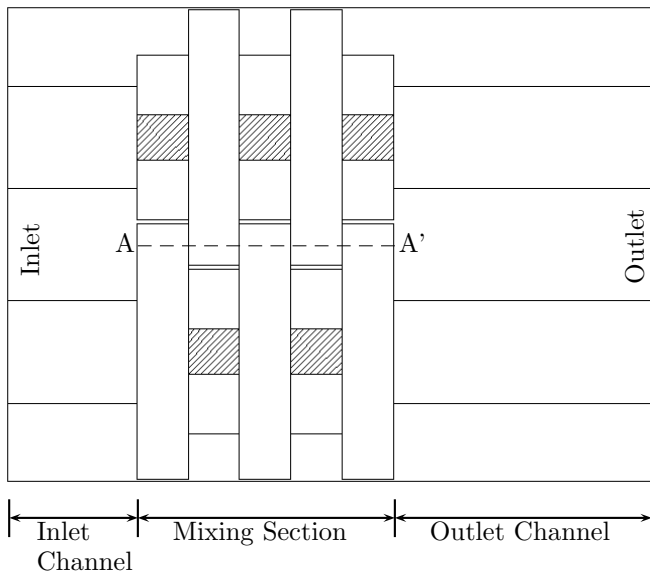
Figure 2: Geometry of the barrel and position of the line AA' in the flow.
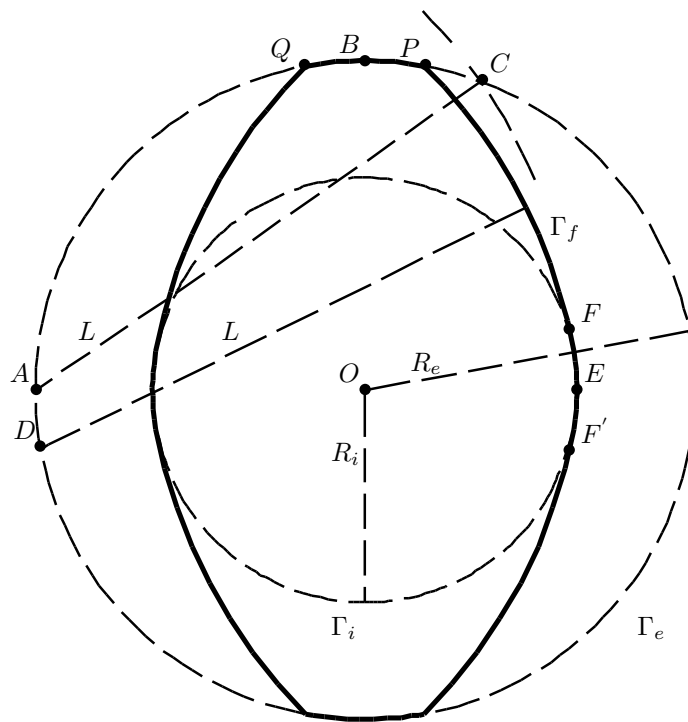
Figure 3: Cross section of one disc of a kneading block
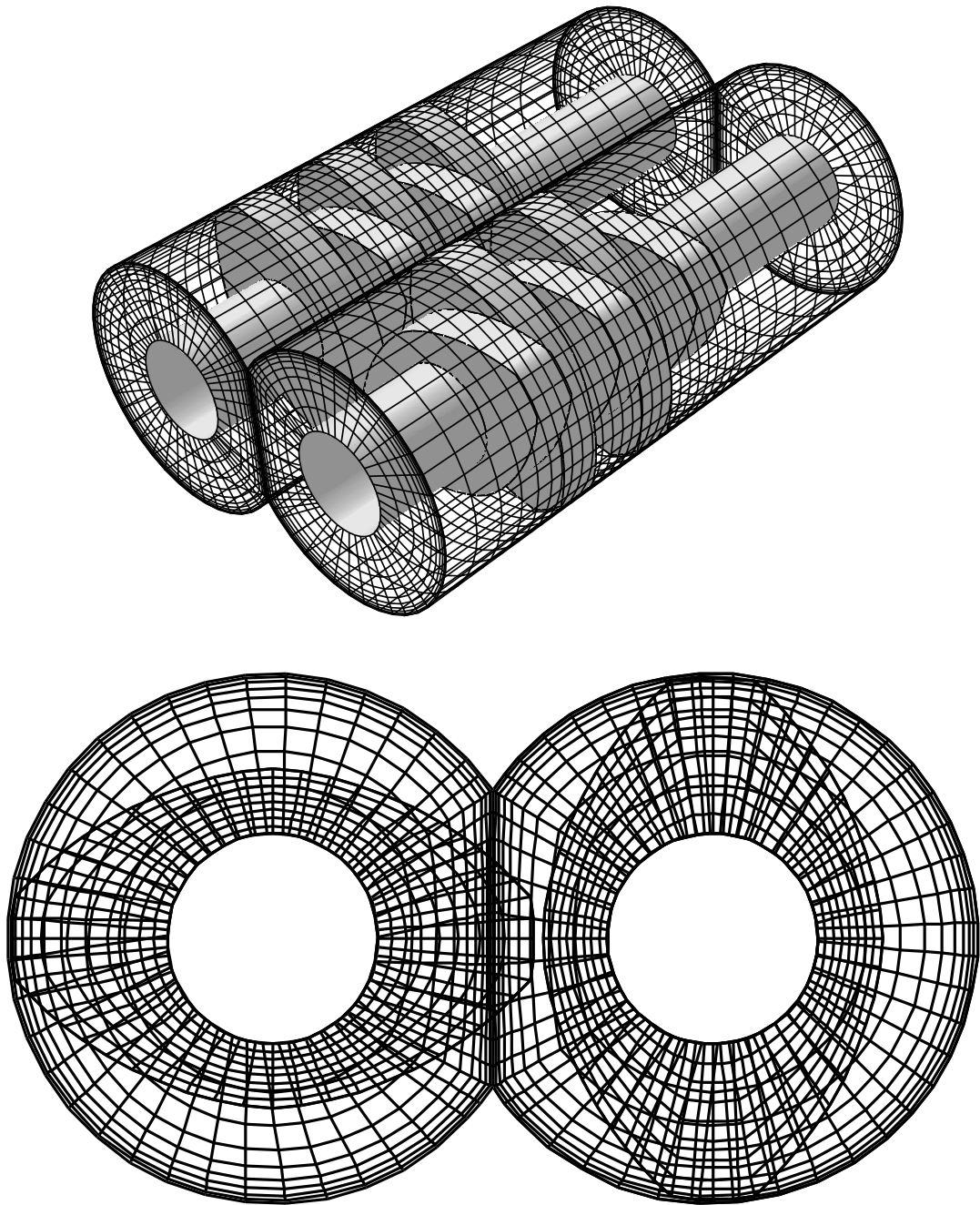
Figure 4: Superposition of the meshes of the barrel and the screws.
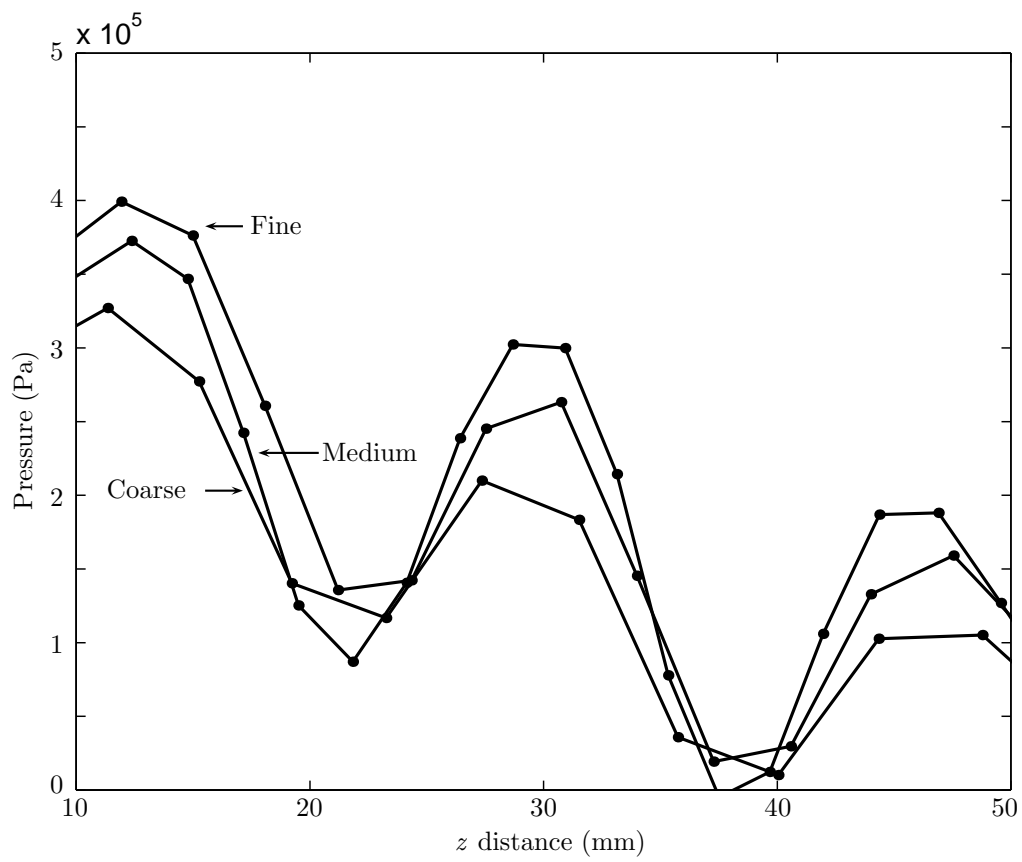
Figure 5: Comparison of the pressure profiles along the line AA' defined in the Figure 2 for three meshes for the neutral element with five discs.
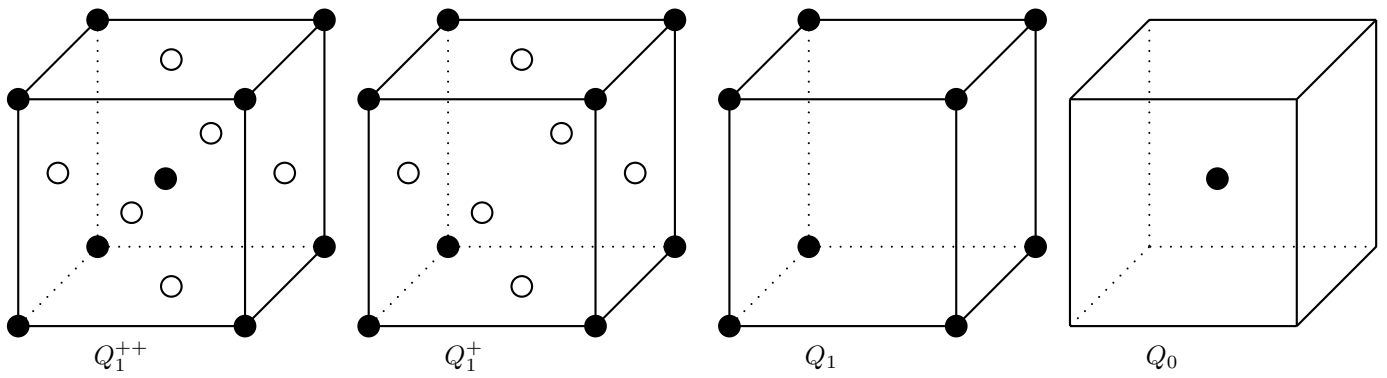
Figure 6: The enriched mini-element (Q_1^{++}), the mini-element (Q_1^{+}), the linear element (Q_1) and the constant element (Q_0). The black dots mean that all components of a vector field are considered as degree of freedom. The white dots mean that only a normal scalar degree of freedom is defined for the considered field.
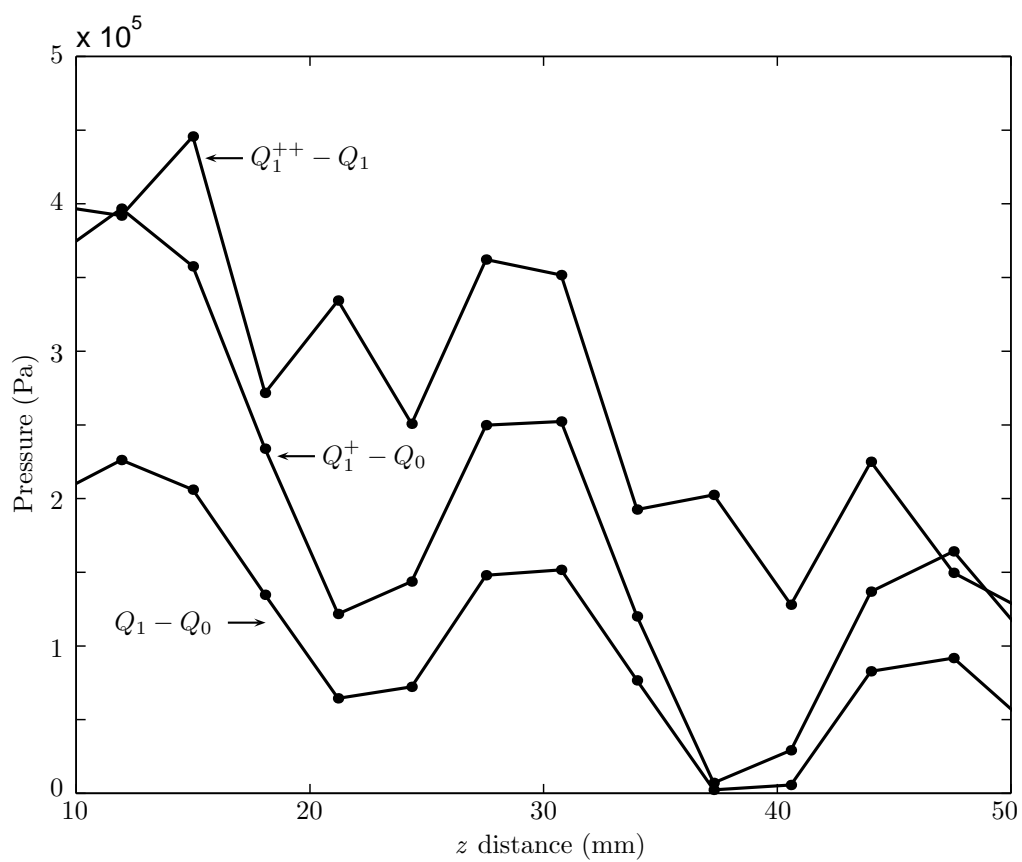
Figure 7: Comparison of the pressure profiles along the line AA' defined in the Figure 2 for three interpolations with the same mesh for the neutral element with five discs.
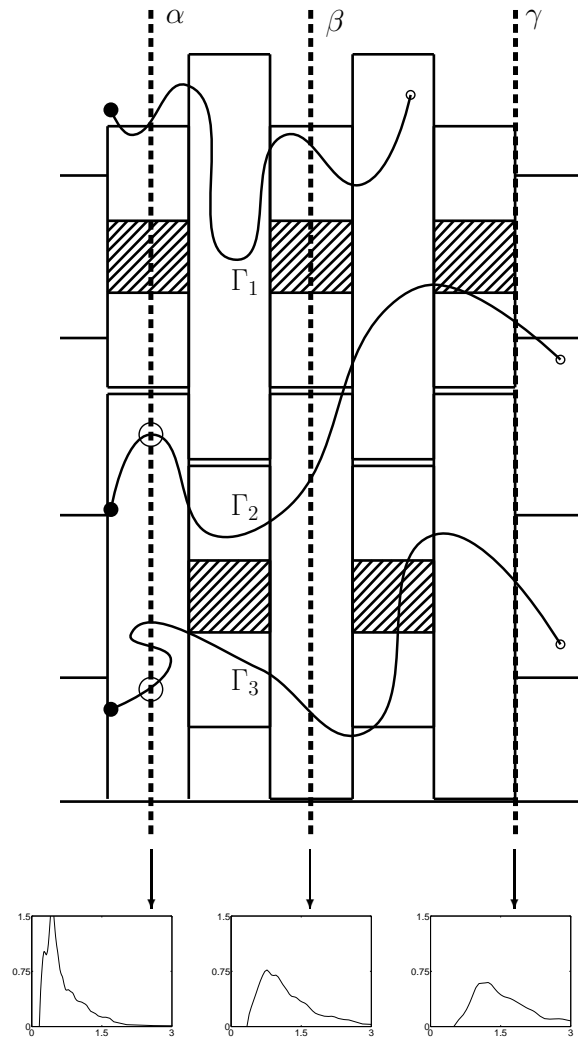
Figure 8: Analysis of the mixing by launching particles from the inlet of the mixing section. Distributions of residence time and total shear are thus obtained along three planes α, β and γ. Several cases are illustrated : the particles stick to the screws (Γ_1), the particles reach the end of the mixing zone in crossing each plane (Γ_2), the particles cut several times the same plane (Γ_3).
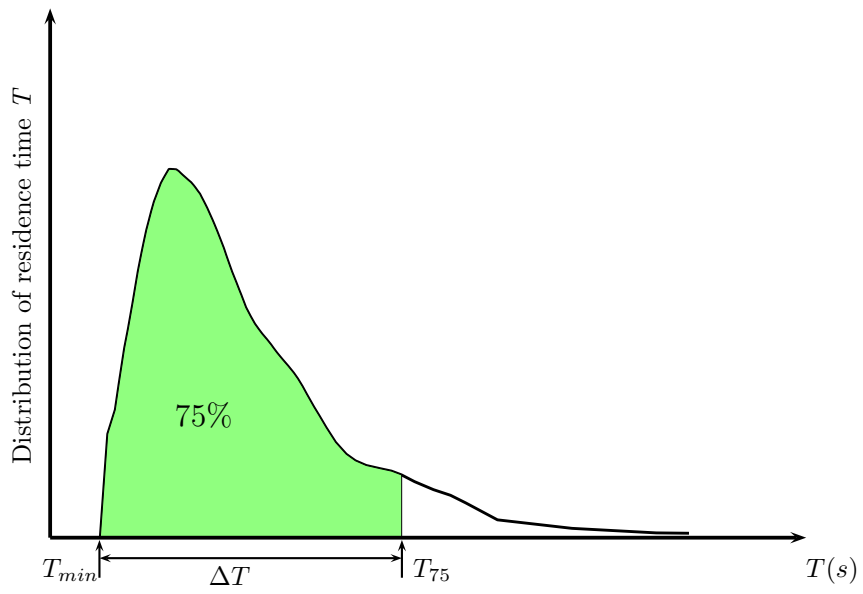
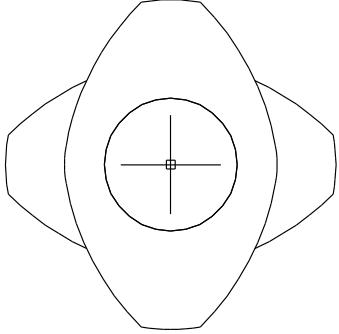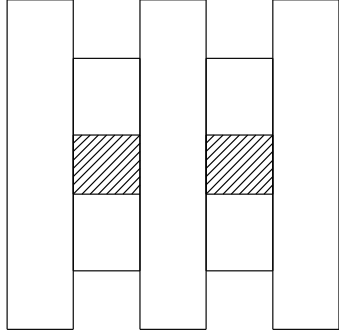Figure 9: Parameters used to characterize the residence time distribution.
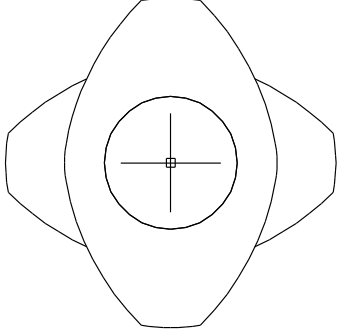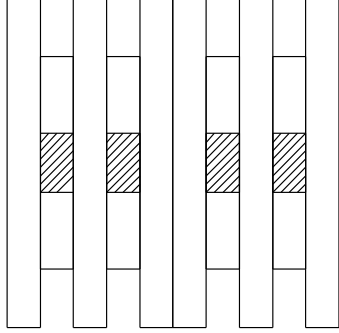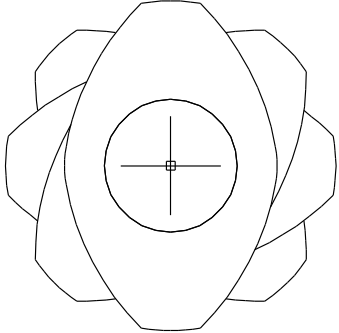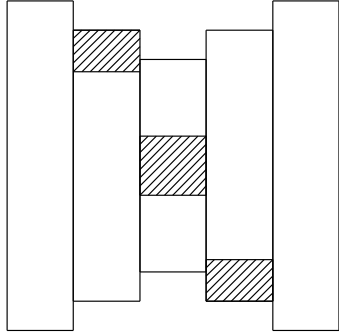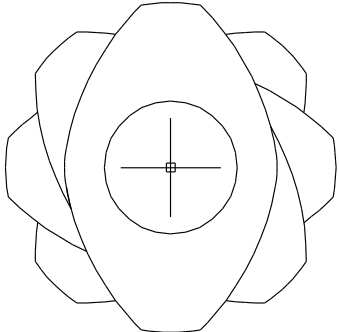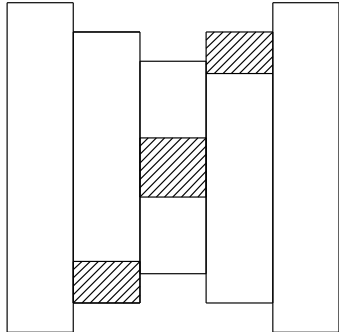
Type of kneading block	Face View	Side view
Neutral element 10 discs $\epsilon = 90°$ length $= 40mm$ (keb 90/10/40)		
Neutral element 5 discs $\epsilon = 90°$ length $= 40mm$ (keb 90/5/40)		
Pump element 5 discs $\epsilon = 45°$ length $= 40mm$ (keb 45/5/40)		
Reverse element 5 discs $\epsilon = -45°$ length $= 40mm$ (keb -45/5/40)		

Figure 10: Configurations of kneading blocks investigated.

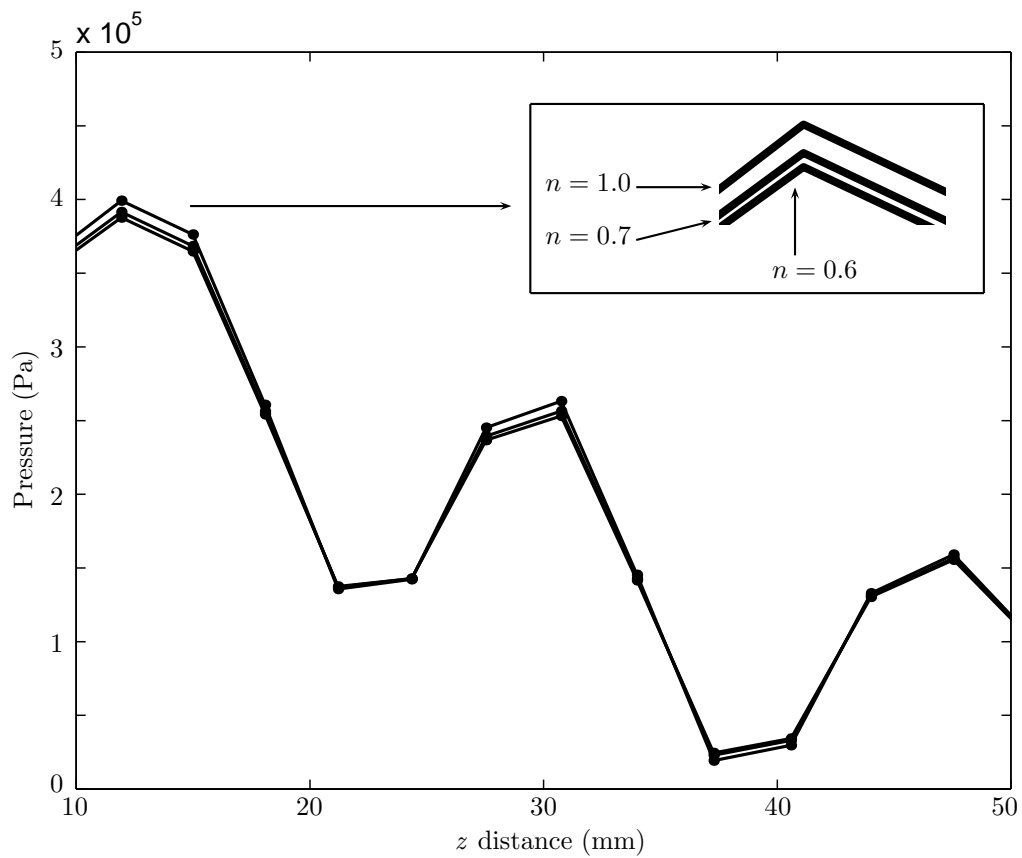Figure 11: Comparison of the pressure profiles along the line AA' defined in the Figure 2 for three values of the power law index for the neutral element with five discs.
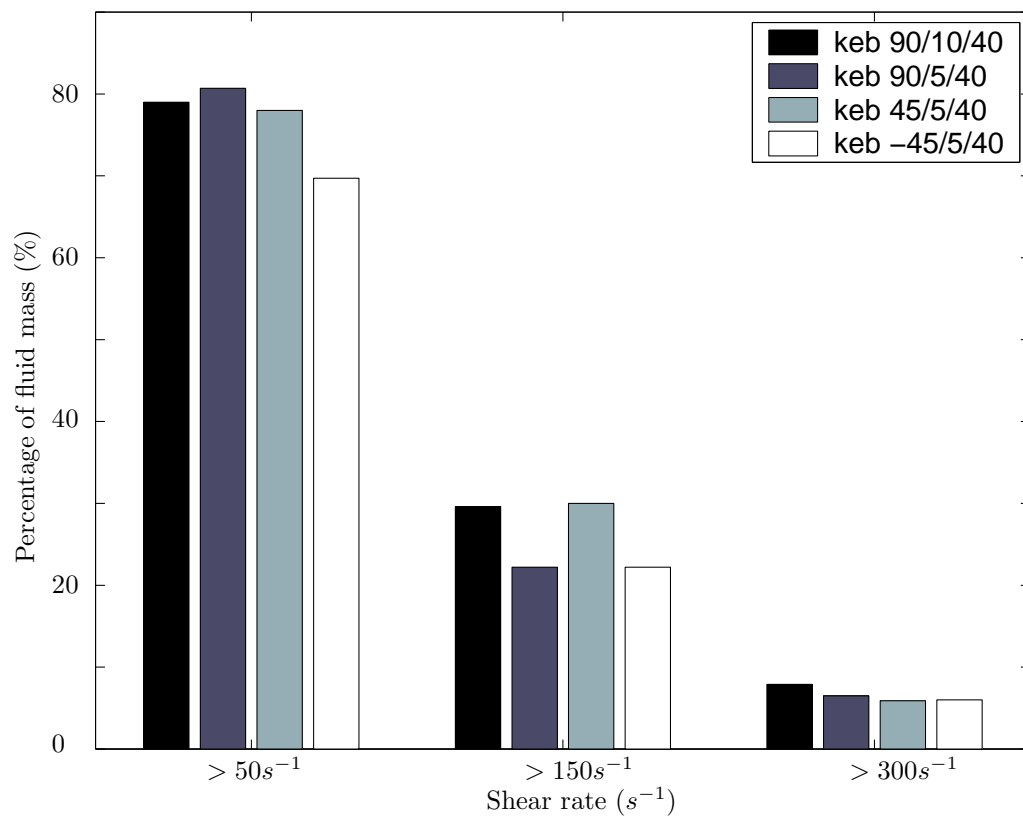
Figure 12: Percentage of fluid mass with a shear rate larger than $50s^{-1}$, $150s^{-1}$ and $300s^{-1}$ respectively.
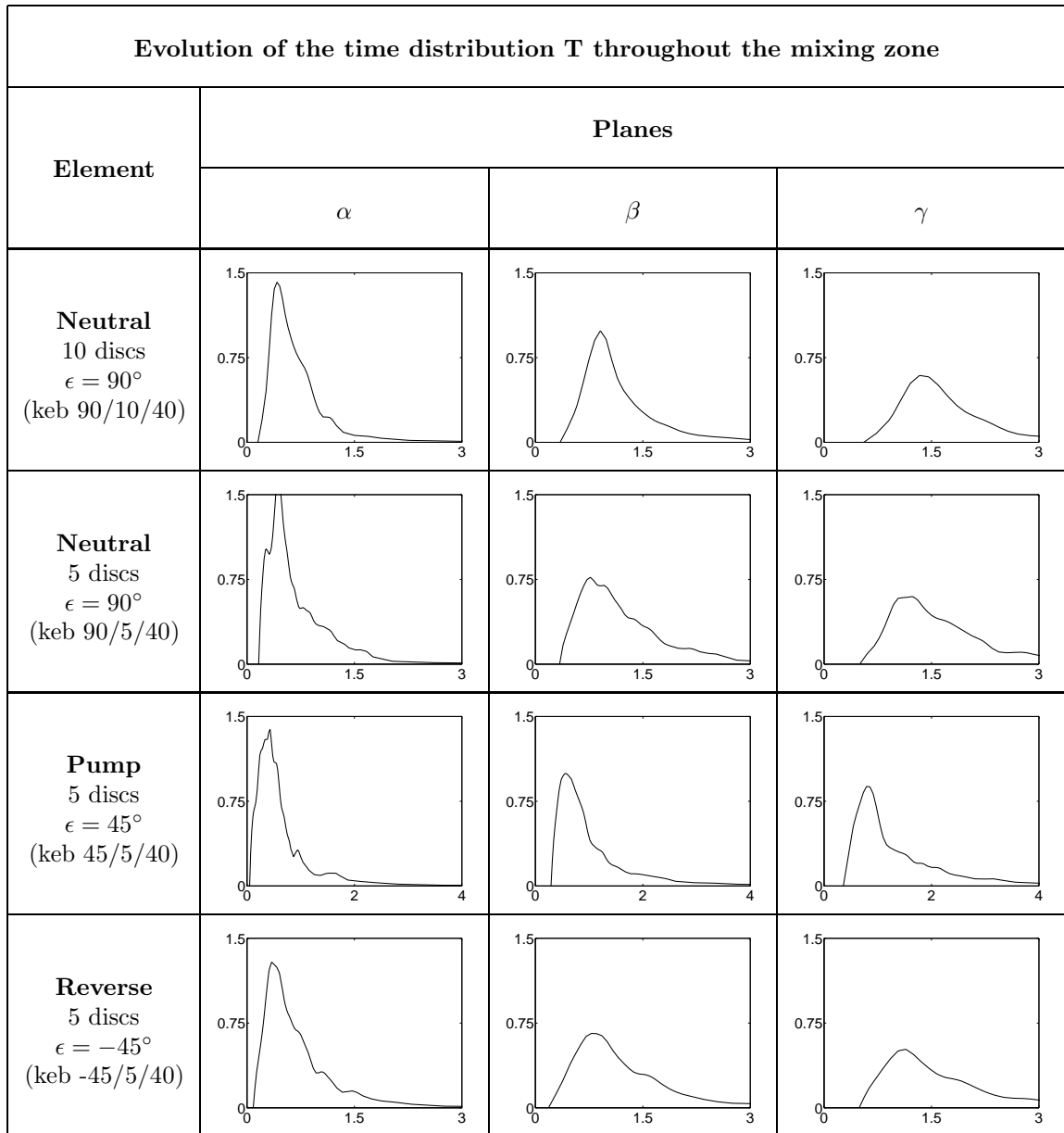
Figure 13: Residence time distributions T in the plane α, β and γ for the different kneading blocks.
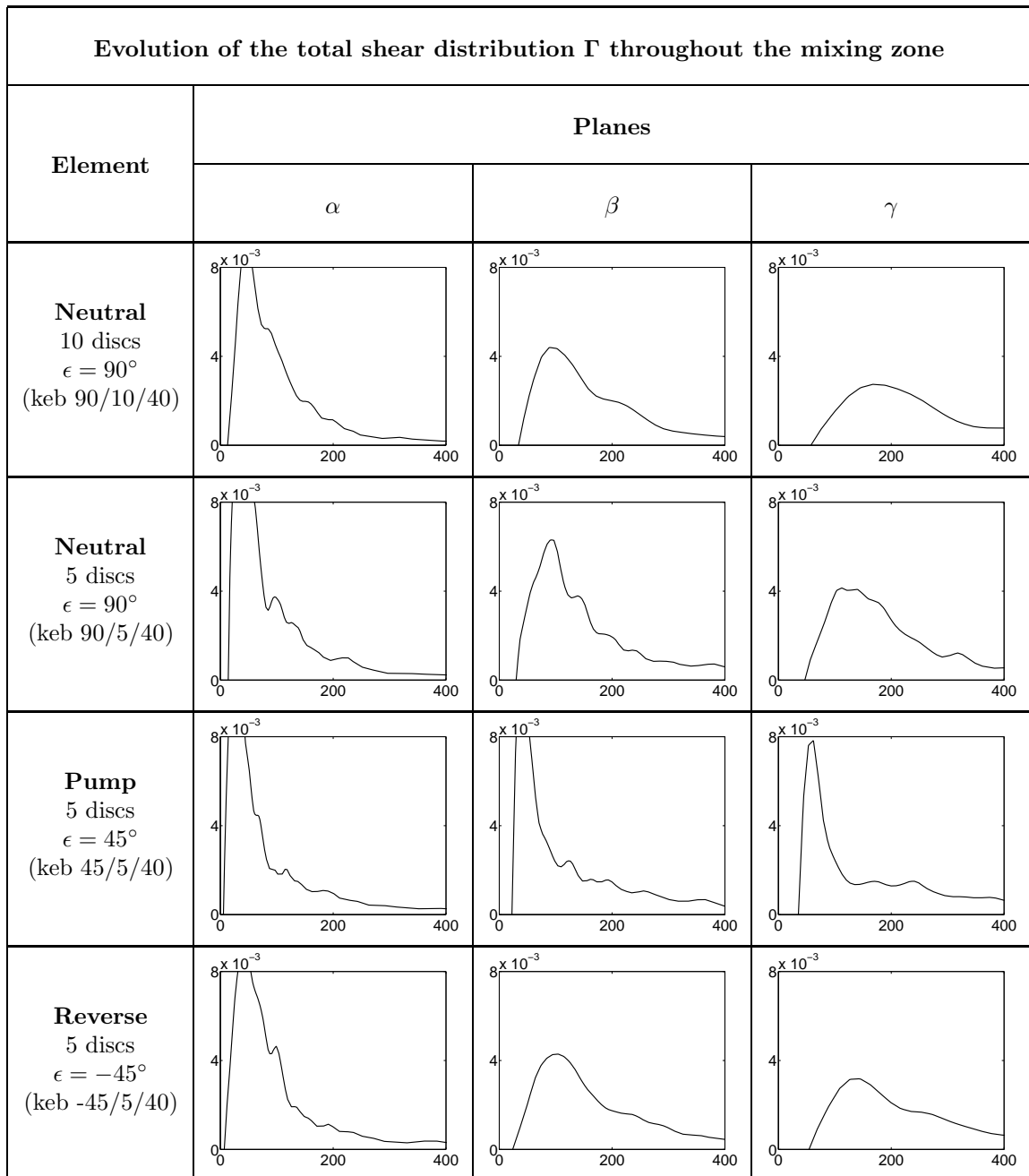
Figure 14: Total shear distributions Γ in the plane α, β and γ for the different kneading blocks.

Dimensions of the barrel (mm)			
Inlet Channel	20.0	Clearance size	0.37
Mixing Section	40.0	Centerline C_L	33.4
Outlet Channel	40.0	Barrel Radius	20.15
Point A	$x = 16.7$, $y = 8.0$, $z = 10.0$		
Point A'	$x = 16.7$, $y = 8.0$, $z = 50.0$		

Table 1: Dimensions of the barrel

Geometrical parameters of the kneading block			
R_e	$19.78mm$	Stagger Angle	$-45°$ or $45°$ or $90°$
R_i	$12.90mm$	Number of disc	5 or 10
L	$32.68mm$	Depth of the disc	$8mm$ or $4mm$
Number of tips	2	Total length	$40mm$

Table 2: Geometrical parameters of the kneading block.

Property	Mathematical definition
Shear rate	$\dot{\gamma} = \sqrt{2\mathbf{d} : \mathbf{d}}$
Total shear	$\Gamma = \int\limits_{0}^{t} \dot{\gamma}\left(t'\right)\, dt'$
Global stretching efficiency in exit section γ	$E = \dfrac{\int\limits_{\gamma} \ln\left(\begin{array}{c} \text{area} \\ \text{stretch} \\ \text{ratio} \end{array}\right)\, dS}{\int\limits_{\gamma} \frac{\Gamma}{\sqrt{2}}\, dS}$

Table 3: Definition of mixing indicators.

Property	Element			
	Neutral 10 discs $\epsilon = 90°$ (keb 90/10/40)	**Neutral** 5 discs $\epsilon = 90°$ (keb 90/5/40)	**Pump** 5 discs $\epsilon = 45°$ (keb 45/5/40)	**Reverse** 5 discs $\epsilon = -45°$ (keb -45/5/40)
Power(W)	602	548	582	618
Pressure drop (Pa) $\Delta p = p_{A'} - p_A$	-3e5	-2.5e5	5e5	-10e5
Residence time(s) T_{75} *Plane α* *Plane β* *Plane γ*	 1.41 3.55 10.4	 1.08 1.58 2.96	 0.92 1.23 2.69	 1.21 1.81 6.67
% of fluid mass with shear rate $> 50s^{-1}$ $> 150s^{-1}$ $> 300s^{-1}$	 79 29.6 7.9	 80.7 22.2 6.5	 78 30 5.97	 69.7 22.2 6
50th **percentile of the maximum of the shear rate in plane γ** (s^{-1})	706	492	431	841
Total shear(-) Γ_{75} *Plane α* *Plane β* *Plane γ*	 242 413 716	 148 224 402	 113 173 377	 228 389 629
Global stretching efficiency in plane γ	4.9e-3	1.3e-2	5.8e-3	5.6e-3

Table 4: Characteristic values for all configurations of kneading blocks.

Property	Element			
	Neutral 10 discs $\epsilon = 90°$ (keb 90/10/40)	**Neutral** 5 discs $\epsilon = 90°$ (keb 90/5/40)	**Pump** 5 discs $\epsilon = 45°$ (keb 45/5/40)	**Reverse** 5 discs $\epsilon = -45°$ (keb -45/5/40)
Residence time (s)				
T_{min}	0.55	0.50	0.36	0.49
ΔT	9.85	2.46	2.33	6.18
Total shear(-)				
Γ_{min}	57	47	36	36
$\Delta\Gamma$	659	355	341	593

Table 5: Analysis of inhomogeneities in term of distribution at the exit section γ.